ADVANCED MATERIALS
www.advmat.de

Selectively Potentiating Hypoxia Levels by Combretastatin A4 Nanomedicine: Toward Highly Enhanced Hypoxia-Activated Prodrug Tirapazamine Therapy for Metastatic Tumors

Shengcai Yang, Zhaohui Tang, Chenyang Hu, Dawei Zhang, Na Shen, Haiyang Yu, and Xuesi Chen**

Hypoxia-activated prodrugs (HAPs) have the potential to selectively kill hypoxic cells and convert tumor hypoxia from a problem to a selective treatment advantage. However, HAPs are unsuccessful in most clinical trials owing to inadequate hypoxia within the treated tumors, as implied by a further substudy of a phase II clinical trial. Here, a novel strategy for the combination of HAPs plus vascular disrupting agent (VDA) nanomedicine for efficacious solid tumor therapy is developed. An effective VDA nanomedicine of poly(L-glutamic acid)-*graft*-methoxy poly(ethylene glycol)/combretastatin A4 (CA4-NPs) is prepared and can selectively enhance tumor hypoxia and boost a typical HAP tirapazamine (TPZ) therapy against metastatic 4T1 breast tumors. After treatment with the combination of TPZ plus CA4-NPs, complete tumor reduction is observed in 4T1 xenograft mice (initial tumor volume is 180 mm^3), and significant tumor shrinkage and antimetastatic effects are observed in challenging large tumors with initial volume of 500 mm^3. The report here highlights the potential of using a combination of HAPs plus VDA nanomedicine in solid tumor therapy.

Tumor hypoxia, a common feature of human and animal solid tumors, is a robust negative clinical biomarker and is considered as one of the best validated therapeutic targets for cancer treatment.[1] On the one hand, tumor hypoxia is a major factor responsible for the failure of many anticancer therapies. On the other hand, tumor hypoxia could be an attractive therapeutic target because it is the basis of a major difference between tumors and normal tissue.[2] Hypoxia-activated prodrugs (HAPs) display selective higher toxicity to hypoxic cells and lower toxicity in higher oxygen tension regions such as normal tissues.[3] Therefore, HAPs have the potential to selectively kill hypoxic cells, thereby converting tumor hypoxia from a problem to a selective treatment advantage.

Tirapazamine (TPZ), a representative HAP, exhibits up to 300-fold higher toxicity under anoxic conditions than under aerobic conditions in vitro in murine and human cancer cell lines.[4] As a prodrug, TPZ can be stimulated to generate transient oxidizing radical intermediates via a single-electron reduction reaction under hypoxic conditions.[5] And the cytotoxic benzotriazinyl (BTZ) radical is obtained via dehydration of TPZ radical intermediates, which can interact with intracellular DNA and cause structural damage to induce apoptosis.[6] However, despite promising phase II clinical trial results, most of the phase III clinical trials failed to show additional benefits of adding TPZ. Nevertheless, a further substudy of data of a phase II clinical trial has demonstrated that TPZ dramatically lowered locoregional failure if patients were selected based on tumor hypoxia.[7] This indicated that the failure of TPZ in clinical trials was mainly due to inadequate hypoxia within the tumors. Thus, all HAP-based strategies will be effective if the tumor hypoxia of patients can be selectively improved.

The hypoxia level of tumors is commonly enhanced by oxygen consumption or vascular occlusion in tumors. For example, the efficient oxygen consumption was achieved by photodynamic therapy (PDT) or sonodynamic therapy (SDT).[8] Alternatively, hepatic artery ligation (HAL) and hypoxia-activated intra-arterial therapy (HAIAT) were used to induce vascular occlusion in tumors.[9] However, HAL and HAIAT can be used only for the hepatocellular carcinoma. Furthermore, PDT, SDT, HAL, and HAIAT are locoregional therapies, and hence these strategies are unsuitable for the treatment of advanced tumors with distant metastasis. Therefore, introduction of a suitable systemic therapy that can specifically enhance the hypoxia level of solid tumors is highly required.

S. Yang, Prof. Z. Tang, Dr. C. Hu, D. Zhang, Dr. N. Shen, H. Yu, Prof. X. Chen
Key Laboratory of Polymer Ecomaterials, Changchun Institute of Applied Chemistry
Chinese Academy of Sciences
Changchun 130022, P. R. China
E-mail: ztang@ciac.ac.cn; xschen@ciac.ac.cn
S. Yang, Prof. X. Chen
College of Chemistry
Jilin University
Changchun 130012, P. R. China
The ORCID identification number(s) for the author(s) of this article can be found under https://doi.org/10.1002/adma.201805955.

DOI: 10.1002/adma.201805955

Vascular disruption also elevates the hypoxia levels, which cuts off the supply source of oxygen.[10] As a representative vascular disrupting agent, combretastatin A4 (CA4) can elicit irreversible vascular shutdown inside tumors.[11] Recently, we developed a CA4-NPs nanomedicine that could selectively disrupt tumor blood vessels and produce significantly low oxyhemoglobin level in solid tumors for at least 48 h after a single intravenous administration.[12] Hence, we reasoned that CA4-NPs can be successfully used to elevate hypoxia levels selectively in tumors and enhance the antitumor efficacy of HAP.

In clinics, most human tumors are discovered only after they have reached a size large enough to be detected. Therefore, strategies that are effective against large tumor burdens have clinical implications.[13] However, the large tumor size presents a number of additional clinically relevant challenges to treatment success, including increased growth rate and a more mature and resistant microenvironment.[14] Successful strategies against these large and aggressive tumors may therefore translate more effectively into positive patient outcomes in the clinic.

In this study, we conducted a proof-of-concept experiment to test the hypothesis of tumor therapy strategies. Therefore, a combination of TPZ plus CA4-NPs was used to treat highly metastatic 4T1 breast carcinoma with initial tumor volume up to 500 mm^3, which emulated stage IV triple-negative breast cancer in human.[15] The CA4-NPs nanomedicines selectively elicited vascular disruption and facilitated heavy hypoxia in tumors (**Scheme 1**). This heavy hypoxia was conducive for the prodrug TPZ activation to a cytotoxic form (BTZ radical) for tumor-specific chemotherapy. Taken together, this rational and convenient strategy led to improved antitumor and antimetastatic efficacies with marginal side effects.

First, the in vitro selective cytotoxic effect of TPZ on 4T1 was determined under simulated normoxic (20% oxygen) or hypoxic (1% oxygen) conditions. As shown in Figure S1a,b in the Supporting Information, TPZ exhibited significantly more cytotoxicity in hypoxic environment than under normoxia. Simultaneously, the hypoxic cytotoxicity ratio (HCR) values at 24 and 48 h were 4.3 and 3.9 (Table S1, Supporting Information), respectively, further confirming its efficacy in hypoxic environment. And the live/dead staining results (Figure S1c, Supporting Information) corroborated the results of the 3-(4,5-dimethyl-2-thiazolyl)-2,5-diphenyl-2*H*-tetrazolium bromide (MTT) assay and highlighted that TPZ required low oxygen tension for complete activation to exert chemotherapeutic activity. Therefore, we reasoned that the improved hypoxia level within tumors is beneficial for enhancing antitumor activity of TPZ in vivo.

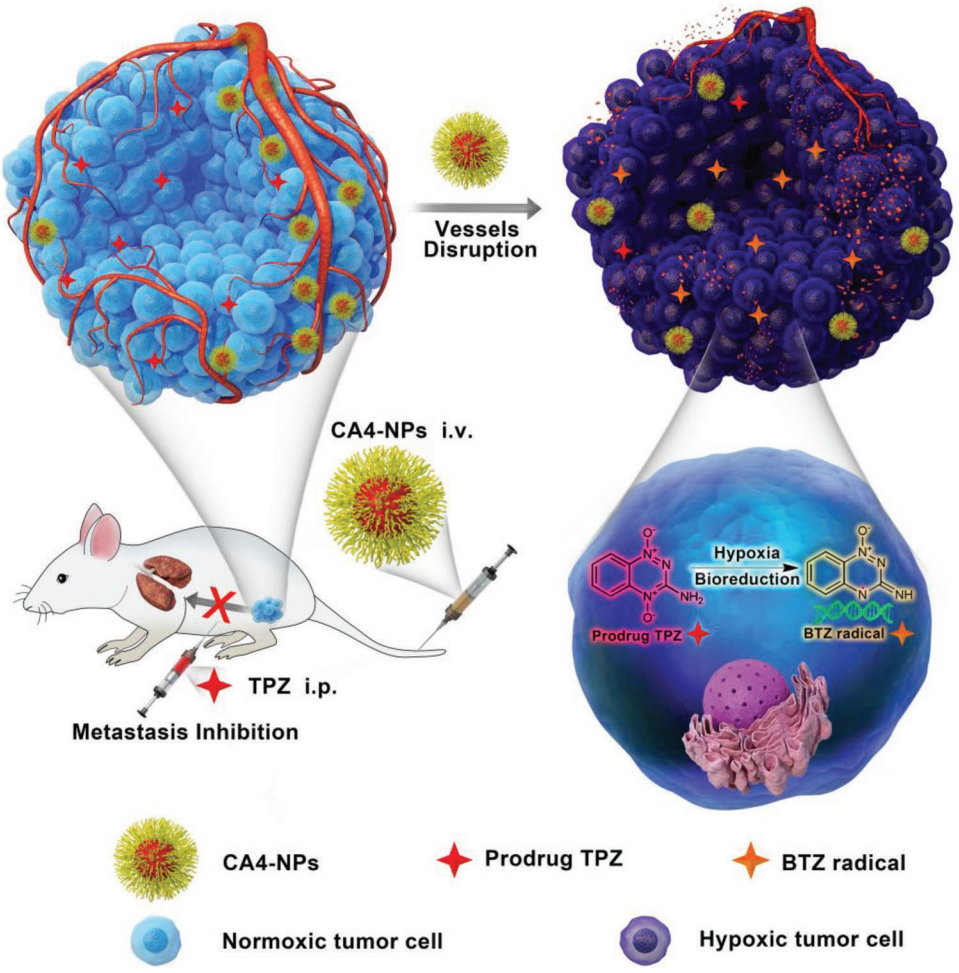

Scheme 1. Schematic illustration of the hypoxia-inducing nanoparticles combined with hypoxia-activated treatment strategy.

Next, we investigated CA4-NPs-mediated hypoxia induction in 4T1 tumor-bearing BALB/c mice. The CA4-NPs was prepared from poly(L-glutamic acid)-*graft*-methoxy poly(ethylene glycol) and CA4 by the Yamaguchi esterification reaction (Figure S2, Supporting Information). The immunohistochemical CD31 staining assay indicated that higher CA4-NPs injection dose resulted in more disruption of tumor vasculature (Figure S3, Supporting Information). Therefore, CA4-NPs was a potential VDA that could destroy tumor blood vessels.

To directly visualize the CA4-NPs-induced hypoxia status within tumors, photoacoustic (PA) imaging and hypoxiaprobe immunofluorescence staining assay were performed for the in vivo studies in 4T1 tumor-bearing mice. PA imaging was utilized to observe hemoglobin (Hb) and oxyhemoglobin (HbO_2) in the blood inside tumors as blue and red signals, respectively (**Figure 1**a). PA imaging was performed at 4 and 24 h postinjection of CA4-NPs, and the scanning area was focused on tumor regions. Oxygen saturation (sO_2) was monitored to reflect hypoxia within tumors (Figure 1c).[16] The sO_2 of the PBS group was 84.0 ± 5.0%, which decreased after intravenous injection of CA4-NPs. Upon prolonging the treatment time from 4 to 24 h, the sO_2 values significantly decreased. These results substantiated that CA4-NPs could induce hypoxia and decrease sO_2 within 4T1 tumors in dose- and time-dependent manners. In addition, no significant sO_2 (83.4 ± 4.2%) change was observed at 24 h postinjection of TPZ compared to the PBS groups (Figure S4, Supporting Information). The sO_2 of the TPZ + CA4-NPs groups was not significantly different from those of CA4-NPs monotherapy at 24 h postinjection, indicating that TPZ did not have any appreciable effect on hypoxia induction. These observations were also confirmed using the hypoxiaprobe staining after systemic administration of identical doses of CA4-NPs via the same administration route and at the same time points (Figure 1b,d; Figure S5, Supporting Information). Moreover, the degree of hypoxia was also determined using immunofluorescence staining of hypoxia-inducible factor 1α (HIF-1α), which was upregulated under hypoxic condition.[17] Compared to the control group, HIF-1α was significantly upregulated in the CA4-NPs treatment groups (Figure S6, Supporting Information). The results of the PA imaging, hypoxiaprobe, and HIF-1α staining assays were strikingly concordant, demonstrating that CA-NPs created profound hypoxia within the tumor microenvironment and cut off the supply source of oxygen within solid tumors. Further investigation of the impact of CA4-NPs on normal tissue confirmed that the hypoxia induced by CA4-NPs selectively occurred inside tumors (Figures S7 and S8, Supporting Information).

The significant upregulation of tumor hypoxia by CA4-NPs provided a strong rationale for studying the therapeutic efficacy of TPZ plus CA4-NPs in a metastatic 4T1 mammary adenocarcinoma model. Mice bearing tumors of moderate sizes (≈180 mm^3) were randomly divided into eight groups: PBS (Group 1), TPZ (40 mg kg^{-1}, Group 2), CA4-NPs (24 mg kg^{-1} on CA4 basis, Group 3), CA4-NPs (36 mg kg^{-1} on CA4 basis, Group 4), CA4-NPs (48 mg kg^{-1} on CA4 basis, Group 5), TPZ + CA4-NPs (40 + 24 mg kg^{-1} on CA4 basis, Group 6), TPZ + CA4-NPs (40 + 36 mg kg^{-1} on CA4 basis, Group 7), and TPZ + CA4-NPs (40 + 48 mg kg^{-1} on CA4 basis, Group 8). Tumor growth was marginally inhibited in free TPZ treatment group compared to the control group (**Figure 2**a), verifying the limited activation of TPZ in solid tumors. Among the CA4-NPs treatment groups (Groups 3, 4, and 5), the monotherapy showed moderate effect on tumor growth inhibition (Table S2, Supporting Information). Consistent with the proposed scenario, combinational therapy with TPZ plus CA4-NPs (Groups 6, 7, and 8) resulted in more suppressed tumor growth in comparison with monotherapy. Notably, Group 8 showed the most efficient therapeutic effect and complete regression of primary tumors on day 10 (Figure 2a,b). To further estimate the therapeutic effects, the excised tumors were processed for hematoxylin and eosin (H&E) and terminal deoxynucleotidyl transferase dUTP nick-end labeling (TUNEL) analyses (Figure 2c). There was no representative staining micrograph in Group 8 owing to the almost complete elimination of tumors. The tumor necrosis and apoptosis areas were calculated thrice in different observation fields (Figure 2d,e). Ample evidence indicates that the combinational strategy of TPZ + CA4-NPs can strongly induce tumor cell apoptosis and suppress tumor growth.

In addition to the antitumor efficacy, the antimetastatic effect of TPZ and CA4-NPs was also evaluated. It has been reported that the 4T1 cancer cells spontaneously disseminate to the lung and liver,[18] so that the lung and liver, as well as primary tumors, were examined for metastasis. In groups treated with PBS or free TPZ, small metastatic nodules were clearly observed in the H&E micrographs of the lung and liver (Figure 2g). In contrast, combinational therapy of TPZ plus CA4-NPs resulted in a substantial reduction of metastatic lesions compared to CA4-NPs monotherapy. Group 8 showed complete suppression of primary tumors with no obvious metastases, suggesting that when combined with CA4-NPs (48 mg kg^{-1} on CA4 basis), TPZ was sufficient to eradicate both primary tumors and metastasis. As matrix metalloproteinase-9 (MMP-9) promotes invasion, metastasis, and survival of 4T1 cells in distant lungs and liver,[19] the MMP-9 expression was also investigated in primary tumors (Figure 2c). Quantitative analysis of these images (Figure 2f) showed that the results of MMP-9 expression also corroborated that the combinational strategy of TPZ + CA4-NPs effectively inhibited primary tumor progression and distant metastasis.

Advanced breast cancer includes five stages (0–IV). Stage IV is critical as it represents metastasis to other sites of the body such as the liver and lung.[20] First, whether mice bearing 4T1 tumors of ≈500 mm^3 had advanced breast cancer was verified. As shown in Figure S9 in the Supporting Information, there were obvious metastatic nodules in the liver and lung, indicating that the mice had stage IV triple-negative breast cancer. Encouraged by the remarkable antitumor results of mice bearing tumors with moderate volumes of ≈180 mm^3, we investigated whether the antitumor effect could be maintained in larger tumors (≈500 mm^3). It was observed that TPZ monotherapy without CA4-NPs had marginal and insignificant efficacy toward tumor regression (**Figure 3**a,c; Table S3, Supporting Information), indicating that CA4-NPs were critical for inducing hypoxia and enhancing TPZ antitumor activity. Compared to CA4-NPs monotherapies (Groups 3, 4, and 5), combination treatments (Groups 6, 7, and 8) exhibited significantly more effective regression of tumor growth. Group 8 also exhibited the most pronounced suppression of tumor growth. The tumor suppression rate was as high as 93.3%, while tumor size shrank to ≈140 mm^3. The H&E and

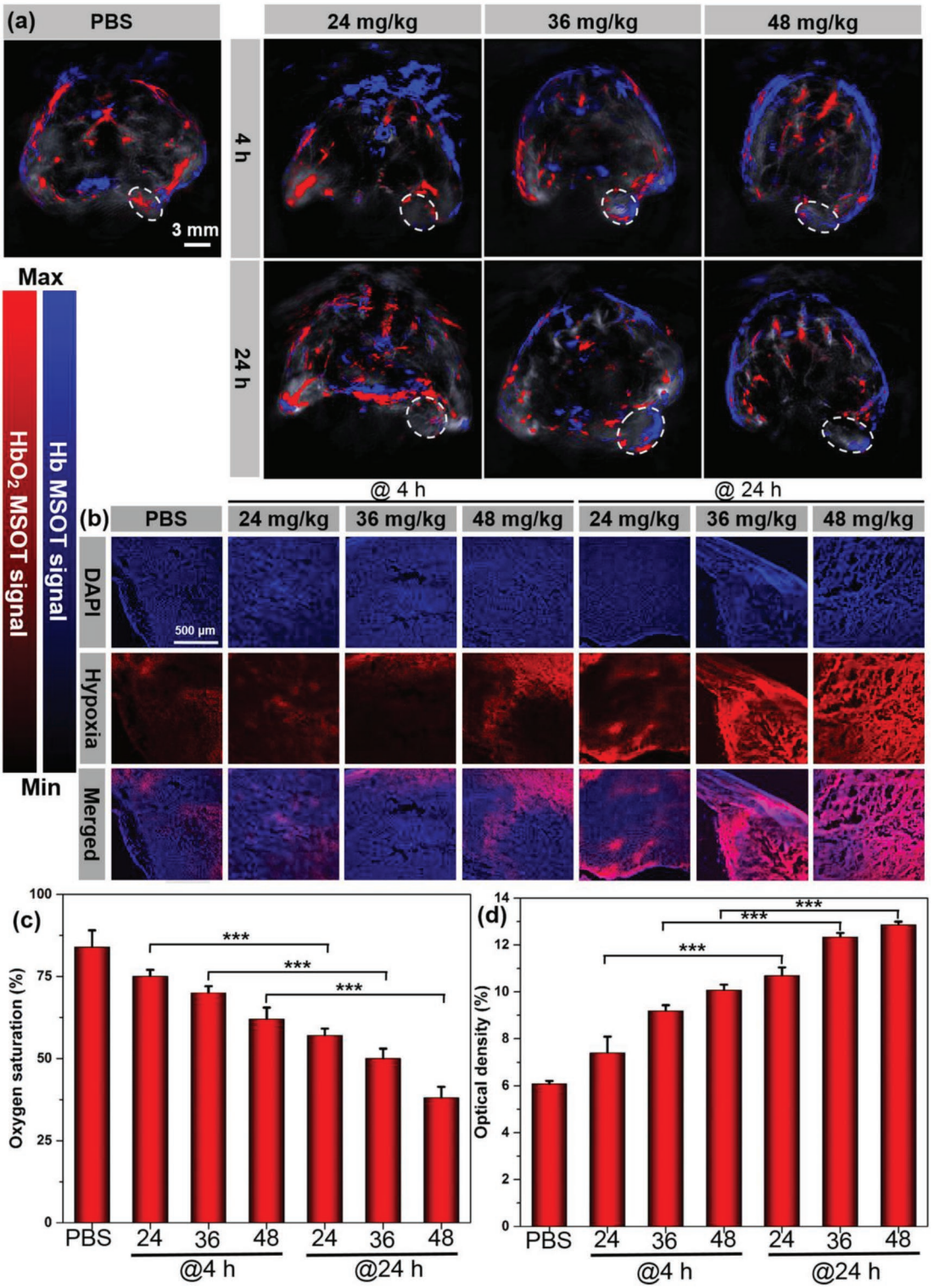

Figure 1. Visualization of hypoxia induced by CA4-NPs in 4T1 tumor-bearing mice. a) PA and b) confocal laser scanning microscopy (CLSM) imaging of hypoxia immunofluorescence staining after intravenous injection of CA4-NPs at 4 and 24 h. White dashed lines represent tumor regions. c) Oxygen saturation within tumors determined from the PA imaging. d) Relative optical densities of tumor sections from hypoxia staining.

TUNEL staining micrograph concurrently revealed that the combinational treatment groups showed higher cell necrotic and apoptosis than monotherapy (Figure 3e,h,i). Taken together, these results further showed that combination treatment not only completely suppressed moderate tumors (≈180 mm^3), but also markedly shrank large tumors (≈500 mm^3).

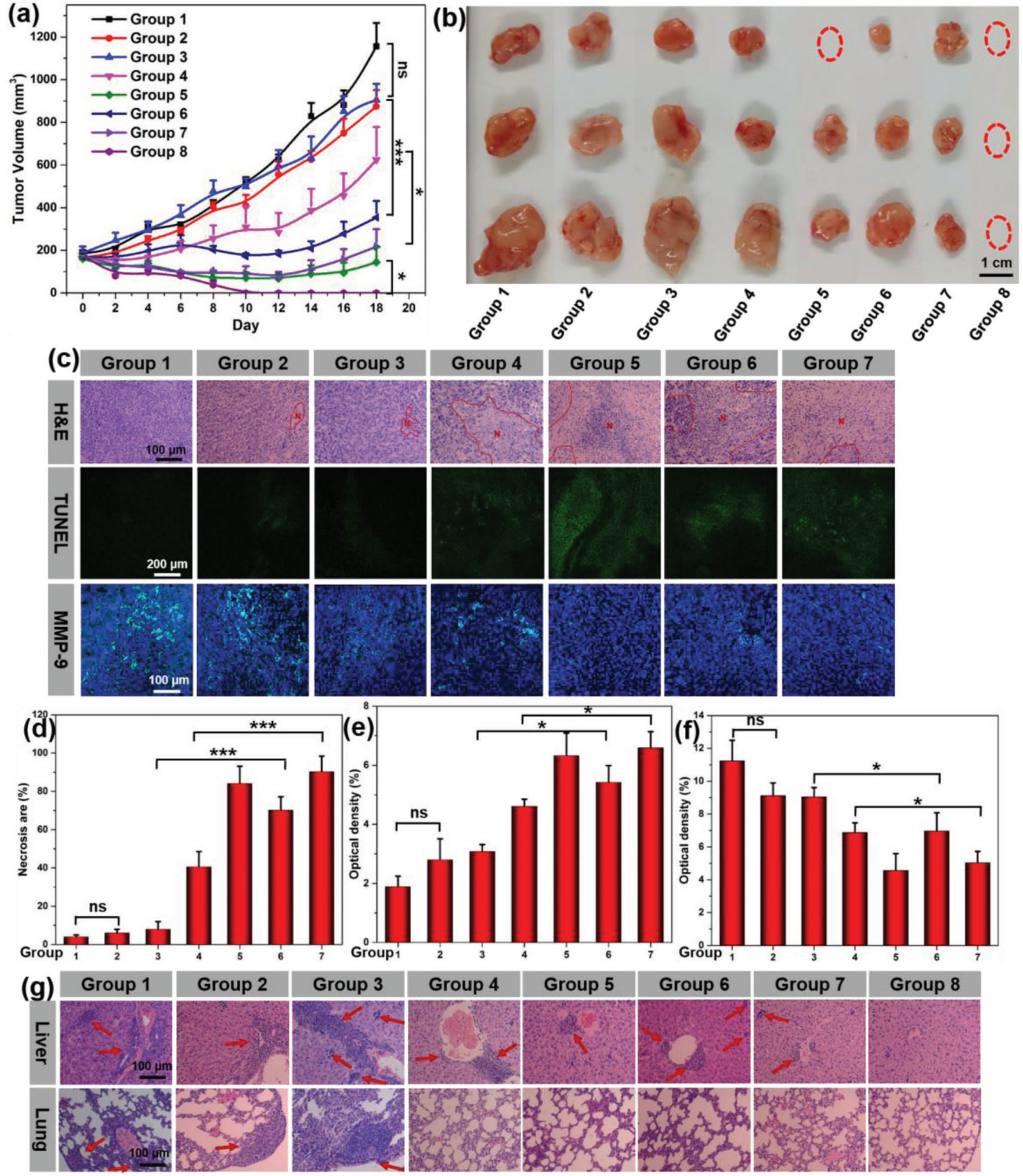

Figure 2. In vivo antitumor and antimetastatic efficacies on BALB/c mice bearing 4T1 tumors with moderate sizes (≈180 mm^3). a) Tumor volume changes of mice during the treatment. b) The representative tumor at the end of the treatment. c) H&E, TUNEL, and MMP-9-stained tumor sections from different treatment groups. "N" represents the necrotic areas. d) Necrotic areas of tumor sections from H&E staining. e) Relative optical densities of tumor sections from TUNEL staining. f) Relative optical densities of tumor sections from MMP-9 staining. g) H&E staining of liver and lung sections from different treatment groups. Red arrow represents micrometastasis. Group 1: PBS; Group 2: TPZ (40 mg kg^{-1}); Group 3: CA4-NPs (24 mg kg^{-1} on CA4 basis); Group 4: CA4-NPs (36 mg kg^{-1} on CA4 basis); Group 5: CA4-NPs (48 mg kg^{-1} on CA4 basis); Group 6: TPZ + CA4-NPs (40 + 24 mg kg^{-1} on CA4 basis); Group 7: TPZ + CA4-NPs (40 + 36 mg kg^{-1} on CA4 basis); Group 8: TPZ + CA4-NPs (40 + 48 mg kg^{-1} on CA4 basis).

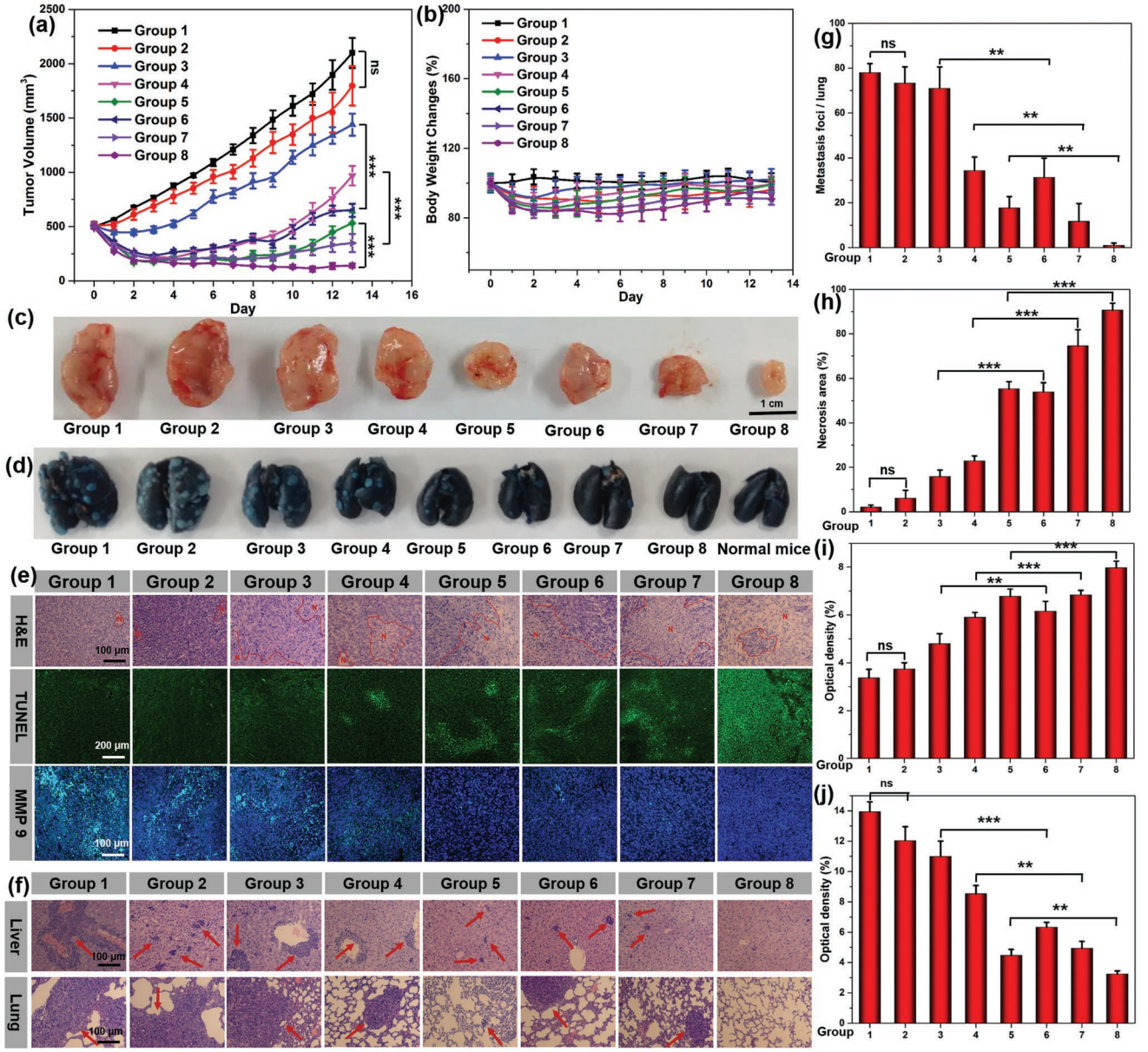

Figure 3. In vivo antitumor and antimetastatic efficacies on BALB/c mice bearing 4T1 tumors with large sizes (≈500 mm^3). a) Tumor volume and b) body weight changes of mice during the treatment. c) The representative tumors and d) lungs at the end of the treatment. e) H&E, TUNEL, and MMP-9-stained tumor sections from different treatment groups. "N" represents the necrotic areas. f) H&E staining of liver and lung sections from different treatment groups. Red arrow represents micrometastasis. g) Number of lung metastases foci from different treatment groups. h) Necrotic areas of tumor sections from H&E. i) Relative optical densities of tumor sections from TUNEL staining. j) Relative optical densities of tumor sections from MMP-9 staining. Group 1: PBS; Group 2: TPZ (40 mg kg^{-1}); Group 3: CA4-NPs (24 mg kg^{-1} on CA4 basis); Group 4: CA4-NPs (36 mg kg^{-1} on CA4 basis); Group 5: CA4-NPs (48 mg kg^{-1} on CA4 basis); Group 6: TPZ + CA4-NPs (40 + 24 mg kg^{-1} on CA4 basis); Group 7: TPZ + CA4-NPs (40 + 36 mg kg^{-1} on CA4 basis); Group 8: TPZ + CA4-NPs (40 + 48 mg kg^{-1} on CA4 basis).

Subsequently, the antimetastatic efficacy of TPZ and CA4-NPs was also studied. To observe pulmonary metastatic nodules, lungs were tracheally injected with India ink and destained in Fekete's solution.[21] The white pulmonary metastasis foci were counted and photographed (Figure 3d,g). The pulmonary metastatic nodules in Group 8 were barely observable and the lung size was normal. Similarly, the H&E staining and MMP-9 expression micrographs showed similar metastasis inhibition (Figure 3e,f,j).

Finally, the long-term safety and systemic toxicity of TPZ plus CA4-NPs were investigated for the possibility of the clinical application. The average body weights of all groups at the end point decreased by <15.0% (Figure S10, Supporting Information; Figure 3b). In addition, no remarkable pathological abnormalities were observed in H&E staining of heart, spleen, and kidney (Figures S11 and S12, Supporting Information). Hematological and biochemical assays were also conducted on day 13. As shown in Figure S13 in the Supporting Information,

the level of white blood cells in Groups 5 and 8 was within the normal range, suggesting no systemic anemia or inflammation occurred after the treatments. In addition, other hematological parameters showed absence of detectable damage as the levels of red blood cells, hematocrit, and hemoglobin were all within the normal ranges. The levels of alanine aminotransferase, blood urea nitrogen, and creatinine were similar to that of normal mice (Figure S14, Supporting Information), further indicating that the combination treatment of TPZ and CA4-NPs had non-systemic toxicity.

In summary, we first developed a combinational strategy with bioreductive TPZ and CA4-NPs for cancer therapy. CA4-NPs were constructed to selectively destroy blood vessels and generate profound hypoxia inside tumors, which was verified by PA imaging and hypoxiaprobe immunofluorescence staining. High hypoxia level is sufficiently strong to potentiate therapeutic and antimetastatic effects of TPZ in a metastatic 4T1 mammary adenocarcinoma model. The combination of TPZ and CA4-NPs showed superior antitumor efficacy over the two monotherapies, highlighting the importance of selectively enhancing hypoxia level within tumors for TPZ therapy. Furthermore, this promising strategy not only completely suppressed moderate tumors (≈180 mm^3), but also markedly shrank large tumors (≈500 mm^3) with distant metastasis. These observations will pave the way for investigating the efficacy of combination treatment with HAP and VDA for other solid tumors.

Supporting Information

Supporting Information is available from the Wiley Online Library or from the author.

Acknowledgements

This work was financially supported by Ministry of Science and Technology of China (Project 2016YFC1100701 and 2018ZX09711003-012) and National Natural Science Foundation of China (Projects 51673189, 51873206, 51673185, 51833010, and 51520105004).

Conflict of Interest

The authors declare no conflict of interest.

Keywords

hypoxia, hypoxia-activated prodrug, metastatic breast carcinoma, nanomedicine, vascular disrupting agent

Received: September 13, 2018
Revised: January 13, 2019
Published online: January 24, 2019

[1] A. Sahu, W. I. Choi, G. Tae, *Adv. Ther.* **2018**, *1*, 1800026.
[2] W. R. Wilson, M. P. Hay, *Nat. Rev. Cancer* **2011**, *11*, 393.
[3] J. M. Brown, W. R. William, *Nat. Rev. Cancer* **2004**, *4*, 437.
[4] a) E. M. Zeman, J. M. Brown, M. J. Lemmon, V. K. Hirst, W. W. Lee, *Int. J. Radiat. Oncol., Biol., Phys.* **1986**, *12*, 1239; b) B.-J. Hong, J. Kim, H. Jeong, S. Bok, Y.-E. Kim, G. O. Ahn, *Radiat. Oncol. J.* **2016**, *34*, 239.
[5] K. O. Hicks, F. B. Pruijn, J. R. Sturman, W. A. Denny, W. R. Wilson, *Cancer Res.* **2003**, *63*, 5970.
[6] M. Birincioglu, P. Jaruga, G. Chowdhury, H. Rodriguez, M. Dizdaroglu, K. S. Gates, *J. Am. Chem. Soc.* **2003**, *125*, 11607.
[7] D. Rischin, R. J. Hicks, R. Fisher, D. Binns, J. Corry, S. Porceddu, L. J. Peters, *J. Clin. Oncol.* **2006**, *24*, 2098.
[8] a) Y. Liu, Y. Liu, W. Bu, C. Cheng, C. Zuo, Q. Xiao, Y. Sun, D. Ni, C. Zhang, J. Liu, J. Shi, *Angew. Chem., Int. Ed.* **2015**, *54*, 8105; b) Q. Feng, Y. Li, X. Yang, W. Zhang, Y. Hao, H. Zhang, L. Hou, Z. Zhang, *J. Controlled Release* **2018**, *275*, 192.
[9] a) W. H. Lin, S. H. Yeh, K. H. Yeh, K. W. Chen, Y. W. Cheng, T. H. Su, P. Jao, L. C. Ni, P. J. Chen, D. S. Chen, *Proc. Natl. Acad. Sci. U. S. A.* **2016**, *113*, 11937; b) R. Duran, S. Mirpour, V. Pekurovsky, S. Ganapathy-Kanniappan, C. F. Brayton, T. C. Cornish, B. Gorodetski, J. Reyes, J. Chapiro, R. E. Schernthaner, C. Frangakis, M. Lin, J. D. Sun, C. P. Hart, J. F. Geschwind, *Clin. Cancer Res.* **2017**, *23*, 536.
[10] M. M. Cooney, W. van Heeckeren, S. Bhakta, J. Ortiz, S. C. Remick, *Nat. Clin. Pract. Oncol.* **2006**, *3*, 682.
[11] G. M. Tozer, C. Kanthou, B. C. Baguley, *Nat. Rev. Cancer* **2005**, *5*, 423.
[12] T. Liu, D. Zhang, W. Song, Z. Tang, J. Zhu, Z. Ma, X. Wang, X. Chen, T. Tong, *Acta Biomater.* **2017**, *53*, 179.
[13] a) J. S. Michaelson, M. Silverstein, J. Wyatt, G. Weber, R. Moore, E. Halpern, D. B. Kopans, K. Hughes, *Cancer* **2002**, *95*, 713; b) A. C. Huang, M. A. Postow, R. J. Orlowski, R. Mick, B. Bengsch, S. Manne, W. Xu, S. Harmon, J. R. Giles, B. Wenz, M. Adamow, D. Kuk, K. S. Panageas, C. Carrera, P. Wong, F. Quagliarello, B. Wubbenhorst, K. D'Andrea, K. E. Pauken, R. S. Herati, R. P. Staupe, J. M. Schenkel, S. McGettigan, S. Kothari, S. M. George, R. H. Vonderheide, R. K. Amaravadi, G. C. Karakousis, L. M. Schuchter, X. Xu, K. L. Nathanson, J. D. Wolchok, T. C. Gangadhar, E. J. Wherry, *Nature* **2017**, *545*, 60.
[14] A. B. Satterlee, J. D. Rojas, P. A. Dayton, L. Huang, *Theranostics* **2017**, *7*, 253.
[15] a) L. C. Bailey-Downs, J. E. Thorpe, B. C. Disch, A. Bastian, P. J. Hauser, T. Farasyn, W. L. Berry, R. E. Hurst, M. A. Ihnat, *PLoS One* **2014**, *9*, e98624; b) P. Kau, G. M. Nagaraja, H. Zheng, D. Gizachew, M. Galukande, S. Krishnan, A. Asea, *BMC Cancer* **2012**, *12*, 120.
[16] H. F. Zhang, K. Maslov, G. Stoica, L. V. Wang, *Nat. Biotechnol.* **2006**, *24*, 848.
[17] J. Rius, M. Guma, C. Schachtrup, K. Akassoglou, A. S. Zinkernagel, V. Nizet, R. S. Johnson, G. G. Haddad, M. Karin, *Nature* **2008**, *453*, 807.
[18] D. M. Brown, E. Ruoslahti, *Cancer Cell* **2004**, *5*, 365.
[19] a) M. Kowanetz, X. Wu, J. Lee, M. Tan, T. Hagenbeek, X. Qu, L. Yu, J. Ross, N. Korsisaari, T. Cao, *Proc. Natl. Acad. Sci.* **2010**, *107*, 21248; b) S. Shen, H. J. Li, K. G. Chen, Y. C. Wang, X. Z. Yang, Z. X. Lian, J. Z. Du, J. Wang, *Nano Lett.* **2017**, *17*, 3822.
[20] L. Bao, A. Haque, K. Jackson, S. Hazari, K. Moroz, R. Jetly, S. Dash, *Am. J. Pathol.* **2011**, *178*, 838.
[21] P. Blezinger, J. J. Wang, M. Gondo, A. Quezada, D. Mehrens, M. French, A. Singhal, S. Sullivan, A. Rolland, R. Ralston, W. Min, *Nat. Biotechnol.* **1999**, *17*, 343.

